View Article Online
View Journal

Dalton Transactions

An international journal of inorganic chemistry

Accepted Manuscript

This article can be cited before page numbers have been issued, to do this please use: A. Ott, W. Leis, M. Seitz and A. Schnepf, *Dalton Trans.*, 2026, DOI: 10.1039/D5DT02489G.

ROYAL SOCIETY OF CHEMISTRY

rsc.li/dalton

View Article Online
DOI: 10.1039/D5DT02489G

ARTICLE

Received 00th January 20xx,
Accepted 00th January 20xx

DOI: 10.1039/x0xx00000x

$[Au_8(TePh)_4dppm_2(Ph_2PCHPPh_2)_2]Cl_2$ a water and air stable red-luminescent gold-tellurolate cluster with an excellent quantum yield

Adrian Ott, Wolfgang Leis, Michael Seitz and Andreas Schnepf*[a]

From the reaction of LiTePh and $dppm(AuCl)_2$ a water and air stable gold-tellurolate cluster featuring a novel core structure can be obtained in good yield. The cluster with the formula $[Au_8(TePh)_4dppm_2(Ph_2PCHPPh_2)_2]Cl_2$ **1** exhibits two Au_4-units with Au-Au distances in the range from 295.4 pm to 335.1 pm. Crystals of **1** show a red luminescence with a high stokes shift and an excellent quantum yield (Φ = 0.28), demonstrating that **1** is a promising red phosphor for pc-LED applications

Introduction

Gold(I) compounds are in the focus of extensive research due to their application as, e.g., antirheumatics,[1] catalysts[2] and photoluminescence compounds.[3] Excimer and exciplex formation in gold(I) molecules, preconditioned by aurophilic interactions is thereby one important aspect for the photoluminescence properties.[4] There are numerous gold complexes which exhibit luminescence with excellent quantum yields up to nearly 100%, but those emit in the high energy spectral range (400-650 nm).[5, 6] For gold complexes emitting in the low energy range (>650 nm), which we perceive as red colour, the quantum yield is significantly lower. This is referred to the energy gap law.[7-9] In this area gold(I)-chalcogenides are the dominant class of substances.[3, 10, 11] The most prominent examples are gold-sulphur and more underrepresented gold-selenium compounds.[10-13] Gold-tellurium compounds, on the other hand, have hardly been investigated, although tellurium is one of the few elements gold forms minerals with in nature, like calaverite ($AuTe_2$), krennerite ($AuTe_2$) and sylvanite ($(Au, Ag)Te_2$).[14-16] Gold-tellurium compounds can be divided in three categories, gold-polytelluride anions,[17-25] gold-tellurides where the Te^{2-} is triply coordinated to three metal atoms,[26-29] and gold-tellurolates, the heavier analogues of thiolates SR, where TeR ligands are present,[30-33]. The tellurolate ligand is thereby either bound to one or two metal atoms.[31] A subgroup of these compounds are polynuclear gold-tellurolate clusters, where the core consists of multiple gold and tellurium atoms.[32] Here, only a few examples of such tellurolates are known for gold, in contrast to the other coinage metals, where numerous examples of copper-tellurolate and silver-tellurolate clusters are known.[13] The known gold tellurolate clusters are those of the composition $(R_3P)_4Au_8(TeR')_8$ (PR_3 =PPh_3, PPh_2Py) (R´= Ph, Tol) which share the same core motif consisting of four gold atoms linearly coordinated by two tellurolates and four gold atoms triply coordinated by two tellurolates and one phosphine ligand (see figure 1).[32] To our knowledge, these clusters are also the only gold-tellurolate compounds exhibiting photoluminescence properties.[32]

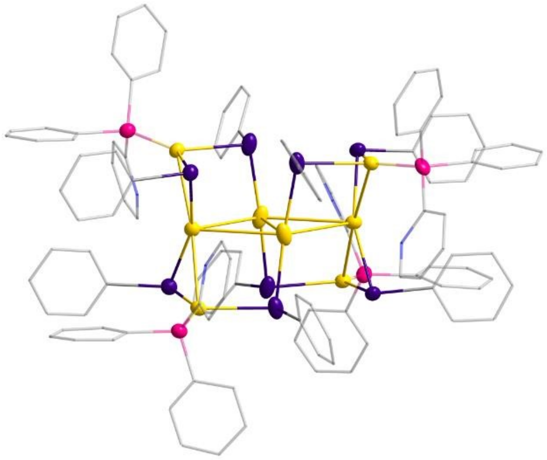

Figure 1: Molecular structure of $[Au_8(TePh)_8(PPh_2Py)_4]$ in the solid state. Hydrogen atoms and solvent molecules are omitted for clarity. Ph and Py groups are displayed as a wire model. Gold (yellow), tellurium (violet), and phosphorus (pink) atoms are shown as thermal ellipsoids with 50% probability.[32]

---

[a] Institute of Inorganic Chemistry, University of Tübingen, Auf der Morgenstelle 18, 72076 Tübingen. Germany. E-Mail: andreas.schnepf@uni-tuebingen.de

†Electronic supplementary information (ESI) available. See DOI: 10.1039/x0xx00000x

View Article Online
DOI: 10.1039/D5DT02489G

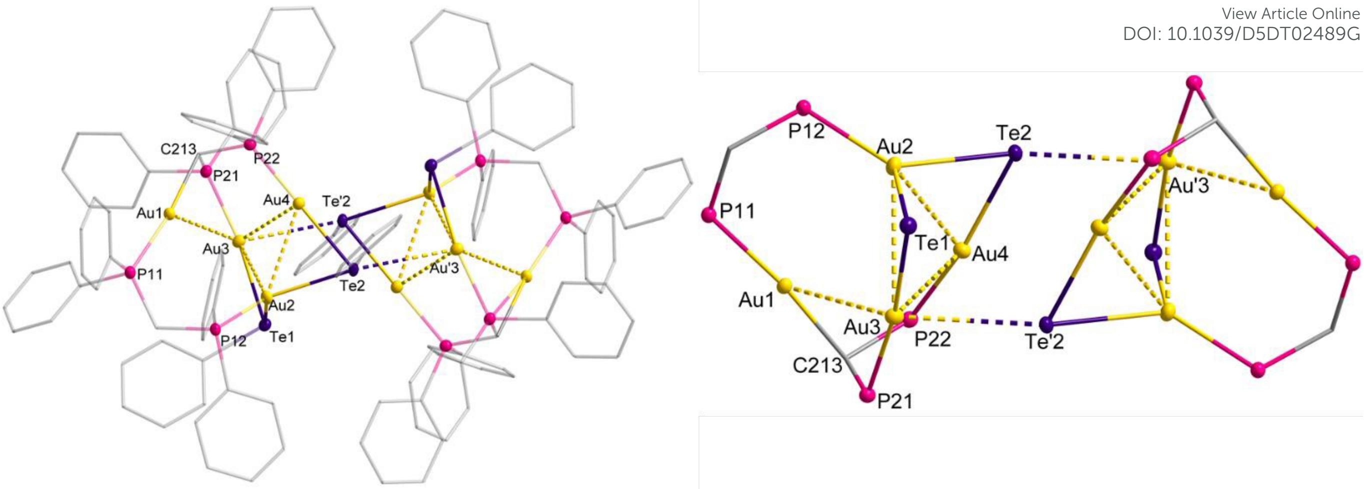

Figure 2: (left) Molecular structure of $[Au_8(TePh)_4dppm_2(Ph_2PCHPPh_2)_2]^{2+}$ within **1** in the solid state. Hydrogen atoms, solvent molecules and chlorides are omitted for clarity. Ph groups are displayed as a wire model. (right) Structure of the core motif; gold (yellow), tellurium (violet), and phosphorus (pink) atoms are shown as thermal ellipsoids with 50% probability. Attractive interactions are shown with dotted lines.

Results and Discussion

In the following we present the gold-tellurolate cluster $[Au_8(TePh)_4dppm_2(Ph_2PCHPPh_2)_2]Cl_2$ **1** (dppm = bis(diphenylphosphino)methane) which is obtained by the reaction of $dppm(AuCl)_2$ and LiTePh in good yield (64 %) as orange crystals. LiTePh is thereby *in situ* prepared from Te_2Ph_2 and L-selectride ($LiB[CH(CH_3)C_2H_5]_3H$). In the ^{31}P-NMR spectrum (in C_6D_6) of the reaction mixture only one signal at 36.0 ppm is observed. However, from the molecular structure (figure 2) it is obvious that four different signals might be expected and thus it is questionable what compound is present in solution prior crystallization. To clarify this, we performed LR-ESI-MS investigations of the $CHCl_3$ solution used for crystallisation (figure S5, supporting information). Thereby a signal at m/z = 1965 is observed, whose isotopic pattern fit to the calculated isotopic pattern of the cation $[Au_4(TePh)_2dppm_2]^+$ (figure S6, supporting information). As only one signal is observed in the ^{31}P-NMR spectrum, this indicates a high dynamic of the phosphine ligands in solution. Additionally, the missing signal of the doubly charged cation $[Au_8(TePh)_4dppm_2(Ph_2PCHPPh_2)_2]^{2+}$ indicates that the formation of the product takes place during crystallization. This is further supported by the fact that **1** is insoluble in water and in organic solvents. In the solid state ^{31}P-NMR spectrum of **1** the expected four signals are observed at $\delta(^{31}P)$: 45.2, 37.6, 32.2, 27.6 ppm (figure S3; supporting information). Thereby, the two downfield shifted signals most likely belong to the two phosphorus atoms of the deprotonated dppm ligand. **1** crystallizes in the triclinic space group $P\overline{1}$ and consists of the cationic cluster $[(dppm)_2(Ph_2P(CH)PPh_2)Au_8(TePh)_4]^{2+}$ and two chloride anions which are each coordinated by three chloroform molecules and one of the acidic hydrogen atoms of the dppm-ligand. **1** was additionally characterised by ^{13}C-ssMAS-NMR, IR and EDX (figures S4, S9, S11-S14; supporting information). A detailed structural view on the bonding situation of the halides can be found in the SI (figure S1; supporting information). The core of the centrosymmetric cluster can be described as a dimer of two Au_4Te_2-units (see figure 2).

Table 1: Selected bond lengths [pm] and bond angles [°]

bond length [pm]		bond angle [°]	
Au1-Au3	335.08(4)	P21-Au3-Te1	172.05(2)
Au1-C213	213.55(31)	P22-Au4-Te2	166.48(2)
Au1-P11	228.98(9)	P12-Au2-Te1	117.33(2)
Au3-P21	229.14(10)	P12-Au2-Te2	134.55(2)
Au4-P22	227.63(10)	Te1-Au2-Te2	101.022(8)
Au2-P12	229.90(8)		

The Au_4Te_2-unit consists of three linearly (Au1, Au3, Au4) and one triply coordinated Au(I) atom (Au2). These units are brought into close proximity by the dipodal dppm ligands, the tripodal deprotonated dppm ligand and two bridging tellurolate ligands. Au1 is linearly coordinated by P11 of the dppm ligand and C213, which is the bridging carbon atom of the deprotonated dppm ligand. The P-Au-C bond angle is 172.6° and the Au1-C213 bond length is 213.6 pm. The phenomenon of dppm ligands undergoing deprotonation to form Au-C bonds is known from the literature.[34] Au3 and Au4 are linearly coordinated, each by the phosphorus atom of the deprotonated dppm ligand and a tellurolate ligand. The bond lengths of Au3-Te1 and Au4-Te2 are 259.8 pm and 258.5 pm, respectively. Au2 is trigonal coordinated from one phosphine and two tellurolates, which is an unusual coordination for gold(I).[35] The Au-Te bond lengths are 273.7 pm (Au2-Te1) and 271.3 pm (Au2-

View Article Online
DOI: 10.1039/D5DT02489G

Te2), and thus considerably longer than the Au-Te bonds to the linearly coordinated gold atoms, which might be due to the higher coordination number of the triply coordinated gold atom. The two Au_4Te_2-units in **1** are connected via attractive interactions of Au3-Te'2 and Au'3-Te2, which have a distance of 328.8 pm, which is significantly larger than the sum of the single-bond covalent radii of Au (124 pm) and Te (136 pm).[36] Hence, both parts are held together by dispersion forces. Within **1,** also a large number of aurophilic interactions are present. Thereby, the distance of Au1 to the nearest gold atom Au3 is, with 335.1 pm, quite long for an aurophilic interaction. The gold atoms Au2, Au3, and Au4 form a nearly isosceles triangle, with Au3-Au2 and Au3-Au4 atom distances of 326.0 pm and 323.5 pm, respectively. The basis of the triangle Au2-Au4 shows an atom distance of 295.4 pm. Such an isosceles Au_3 triangle motif is also observed within the cluster $Au_8(TePh)_8(PPh_2Py)_4$. There the Au_3 triangle motifs share the same basis with a short Au-Au distance of 295.2 pm and longer distances of the legs of the triangles of 325.0 pm and 330.1 pm comparable to **1**.[32] Also the Au-Te bond lengths in $[Au_8(TePh)_8(PPh_3)_4]$ are similar to those found in **1.** Interestingly, crystals of **1** show a bright red luminescence under UV-light as discussed in the following.

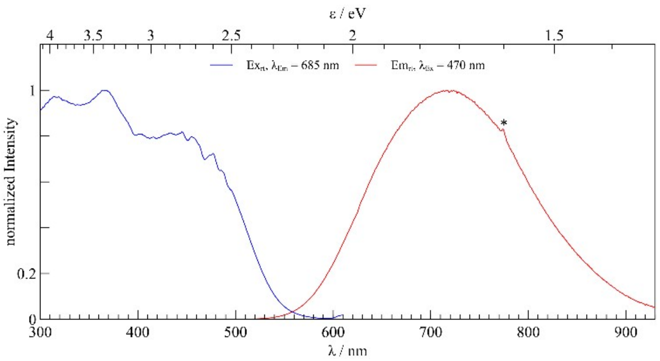

Figure 3: (left) Normalized photoluminescence excitation (PLE (blue)) and emission (PL (red)) spectra of **1** in the solid state at room temperature. PLE was recorded with λ(em) = 685 nm and PL with λ(exc) = 470 nm.

In the solid state, **1** exhibits a broad emission band with a maximum at 715 nm, after excitation at 470 nm. The excitation spectrum shows that the excitation maximum is at 371 nm with emission detection at 685 nm (figure 3). The luminescence lifetime in the presence of oxygen, measured at 685 nm, is obtained from a bi-exponential fit yielding lifetimes of 2.3 µs (46 %) and 1.1 µs (54 %). The lifetime changes only slightly to 2.2 µs (25 %) and 0.9 µs (75 %) when switching to an inert argon atmosphere. It cannot be said with certainty whether this is phosphorescence, but the lifetime and Stokes shift suggest that it is, while the fact that oxygen hardly changes the lifetime suggests that it is not. The quantum yield amounts to $\Phi = 0.28$ at room temperature in the solid state in the presence of oxygen. The quantum yield at higher wavelengths is normally lower because of the energy gap law.[8, 9] A similar emission maximum of 705 nm is known from the complex $[Au(^{Dipp}PZI)(DMAC)]$ (^{Dipp}PZI = 1,3-bis(2,6-diisopropylphenyl)pyrazinoimidazolium) (DMAC = dimethylacridinide), however, with a lower quantum yield of $\Phi = 0.10$.[7] An example for a thiolate protected gold cluster is $Au_{24}(SCH_2C_6H_4{}^tBu)_{20}$ which has an emission maximum at 657 nm with a quantum yield of $\Phi = 0.02$.[37] Additionally, a red-emitting heterometallic phosphine protected ruthenium-gold cluster with an even higher quantum yield of $\Phi = 0.37$ that emits at 720 nm is known. However, in this compound the photoluminescence is almost completely quenched by O_2.[38] This is not the case for **1**, which shows a bright photoluminescence in the presence of oxygen. Consequently, the only gold-tellurolate compounds reported to show photoluminescence are the $(R_3P)_4Au_8(TeR')_8$ clusters and **1**. Both compounds exhibit similar Au_3-triangle motifs with nearly identical bond lengths. However, the emission of **1** is 45 nm red-shifted in comparison to the luminescence of the $[Au_8(TePh)_8(PPh_3)_4]$ cluster in the solid state (λ_{max} = 660 nm).[32] Additionally, solid **1** is stable up to 153 °C. Beyond this temperature the cluster decomposes (figure S10, supporting information). **1** can be stored under air for months without

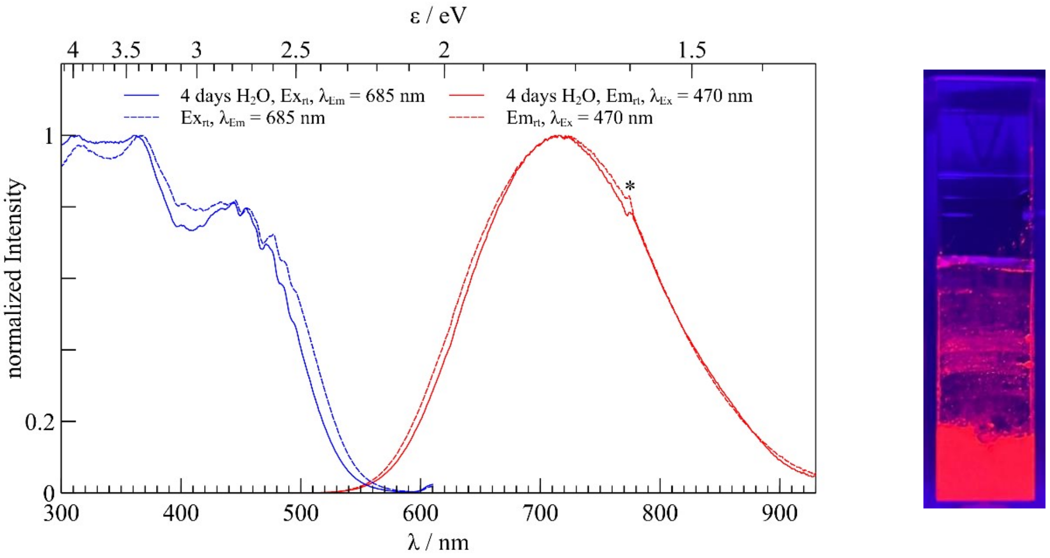

Figure 4: (left) Normalized photoluminescence excitation (PLE (blue)) and emission (PL (red)) spectra of **1** in the solid state at room temperature before (dashed) and after 4 days immersed in H_2O (solid). PLE was recorded with λ(em) = 685 nm and PL with λ(exc) = 470 nm. (right) cuvette with grinded powder of **1** with added water

View Article Online
DOI: 10.1039/D5DT02489G

decomposition. When crystals of **1** are grinded and put under water for two weeks no decomposition is visible (figure 4 (right)). Additionally, the excitation and emission spectra of **1** were recorded before and after it was immersed for 4 days in water (figure 4 (left)). Thereby a comparison of the excitation spectra after water immersion shows a small hypsochromic shift. Comparing the emission spectra a small and seemingly asymmetric change in the band shape is obvious, but no significant shift of the maximum. This stability of **1** is atypical for gold tellurium compounds, which usually decompose at room temperature, as evidenced by a precipitation of elemental tellurium. This stability, in addition to the discussed optical properties, demonstrate that **1** is a promising red phosphor for pc-LED applications, since for this a high thermal stability and chemical resistance is required (figure S15, supporting information).

Conclusions

We presented the synthesis, structure and luminescence properties of a new gold(I)-tellurolate cluster, with a remarkable stability against water and air. The bright red luminescence at 715 nm, with a quantum yield of $\Phi = 0.28$, combined with the high stability renders the cluster as a promising phosphor for pc-LED applications. It also demonstrates the value of further investigating the underrepresented chemistry and properties of gold(I)-tellurolate clusters. Thereby, by changing the phosphines and tellurolates it is maybe possible to render the emission wavelength, the solubility, and further increase the quantum yield for applications of those compounds in various other fields.

Experimental Details

Starting material:
The starting material, Ph_2Te_2[39] and dppm$(AuCl)_2$[40] were prepared according to literature. The other chemicals were commercially available.

Preparation of [(dppm)$_2$(Ph$_2$P(CH)PPh$_2$)Au$_8$(TePh)$_4$]Cl$_2$ (1):
Ph_2Te_2 (0.205 g, 0.5 mmol) is dissolved in 20 mL anhydrous THF. $LiB[CH(CH_3)C_2H_5]_3H$ (L-selectride) 1 M in THF (1 mL, 1 mmol) is added and the mixture is stirred for 1 h at room temperature. [dppm$(AuCl)_2$] (0.425 g, 0.5 mmol) is added to the yellow solution and the reaction is stirred for 1 h, afterward the solvent is removed in a vacuum. The resulting orange solid is dissolved in 15 mL chloroform and filtered with a 0.2 µm syringe filter. After a few days orange crystals are obtained through slow evaporation of the solvent in an open vessel. The remaining chloroform is filtered off and the remaining crystals are washed three times with n-pentane, and dried in a vacuum. The product is obtained as orange crystals of **1**.: Yield: (396 mg, 0,05 mmol, 64% (Yield based on gold)). Analytical data:

31P-CP/MAS-NMR (300 MHz, 6000 Hz): δ [ppm] = 45.2, 37.6, 32.2, 27.6. (figure S3, supporting information)
13C-CP/MAS-NMR (300 MHz, 6000 Hz): δ [ppm] = 138.0, 136.5, 136.0, 134.0, 132.6, 132.1, 131.0, 130.2, 129.8, 128.9, 127.6, 126.5, 112.0, 110.9, 82.4, 32.1. (figure S4, supporting information)

Conflicts of interest

There are no conflicts to declare

Data availability

The data supporting this article have been included as part of the ESI. †
Crystallographic data for this paper has been deposited at the CCDC (Deposition number 2483370).

Acknowledgements

The authors thank Claudio Schrenk for conducting the single-crystal X-Ray structure determination, Klaus Eichele for conducting the ssMAS-NMR measurements, Markus Ströbele for conducting the DTA/TG Analysis and Elke Nadler for conducting the EDX and REM measurements.

Notes and references

1 J. Aaseth, M. Haugen and Ø. Førre, *Analyst*, 1998, **123**, 3-6.
2 A. S. K. Hashmi and G. J. Hutchings, *Angew. Chem., Int. Ed.*, 2006, **45**, 7896-7936.
3 X. He and V. W.-W. Yam, *Coord. Chem. Rev.*, 2011, **255**, 2111-2123.
4 H. Schmidbaur and H. G. Raubenheimer, *Angew. Chem., Int. Ed.*, 2020, **59**, 14748-14771.
5 M. Baron, C. Tubaro, A. Biffis, M. Basato, C. Graiff, A. Poater, L. Cavallo, N. Armaroli and G. Accorsi, *Inorg. Chem.*, 2012, **51**, 1778-1784.
6 V. R. Naina, S. Gillhuber, C. Ritschel, D. Jin, Shubham, S. Lebedkin, C. Feldmann, F. Weigend, M. M. Kappes and P. W. Roesky, *Angew. Chem., Int. Ed.*, 2025, **64**, e202414517.
7 S. Avula, B. H. Jhun, U. Jo, S. Heo, J. Y. Lee and Y. You, *Adv. Sci.*, 2024, **11**, 2305745.
8 J. A. Treadway, B. Loeb, R. Lopez, P. A. Anderson, F. R. Keene and T. J. Meyer, *Inorg. Chem.*, 1996, **35**, 2242-2246.
9 J. V. Caspar and T. J. Meyer, *J. Phys. Chem.*, 1983, **87**, 952-957.
10 E. R. T. Tiekink and J.-G. Kang, *Coord. Chem. Rev.*, 2009, **253**, 1627-1648.
11 J. M. Forward, D. Bohmann, J. P. Fackler Jr and R. J. Staples, *Inorg. Chem.*, 1995, **34**, 6330-6336.
12 O. Crespo, M. C. Gimeno, A. Laguna, M. Kulcsar and C. Silvestru, *Inorg. Chem.*, 2009, **48**, 4134-4142.
13 O. Fuhr, S. Dehnen and D. Fenske, *Chem. Soc. Rev.*, 2013, **42**, 1871-1906.
14 K. Balzuweit, H. Meekes and P. Bennema, *J. Phys. D: Appl. Phys.*, 1991, **24**, 203.
15 G. Tunell and C. Ksanda, *J. Wash. Acad. Sci.*, 1936, **26**, 507-509.
16 G. Tunell, *Am. Min.*, 1941, **26**, 457-477.

View Article Online
DOI: 10.1039/D5DT02489G

17 R. Haushalter, *Inorg. Chim. Acta*, 1985, **102**, L37-L38.
18 R. C. Haushalter, *Angew. Chem., Int. Ed. Engl.*, 1985, **24**, 432-433.
19 S. M. Dibrov and J. A. Ibers, *Commun. Chem.*, 2003, DOI: 10.1039/B306415H, 2158-2159.
20 S. S. Dhingra and R. C. Haushalter, *Inorg. Chem.*, 1994, **33**, 2735-2737.
21 C. Wang and R. C. Haushalter, *Inorg. Chem.*, 1999, **38**, 595-597.
22 S. S. Dhingra, D. K. Seo, G. R. Kowach, R. K. Kremer, J. L. Shreeve-Keyer, R. C. Haushalter and M. H. Whangbo, *Angew. Chem., Int. Ed. Engl.*, 1997, **36**, 1087-1090.
23 D. M. Smith, L. C. Roof, M. A. Ansari, J. M. McConnachie, J. C. Bollinger, M. A. Pell, R. J. Salm and J. A. Ibers, *Inorg. Chem.*, 1996, **35**, 4999-5006.
24 C. J. Warren, D. M. Ho, A. B. Bocarsly and R. C. Haushalter, *J. Am. Chem. Soc.*, 1993, **115**, 6416-6417.
25 M. A. Ansari, J. C. Bollinger and J. A. Ibers, *J. Am. Chem. Soc.*, 1993, **115**, 3838-3839.
26 K. Angermaier and H. Schmidbaur, *Z. Naturforsch. B*, 1996, **51**, 879-882.
27 A. M. Polgar, F. Weigend, A. Zhang, M. J. Stillman and J. F. Corrigan, *J. Am. Chem. Soc.*, 2017, **139**, 14045-14048.
28 J. Olkowska-Oetzel, P. Sevillano, A. Eichhöfer and D. Fenske, *European Journal of Inorganic Chemistry*, 2004, **2004**, 1100-1106.
29 B. J. Frogley, A. F. Hill, C. S. Onn and L. J. Watson, *Angew. Chem., Int. Ed.*, 2019, **58**, 15349-15353.
30 E. S. Lang, C. Maichle-Mössmer and J. Strähle, *Z. Anorg. Allg. Chem.*, 1994, **620**, 1678-1685.
31 P. J. Bonasia, D. E. Gindelberger and J. Arnold, *Inorg. Chem.*, 1993, **32**, 5126-5131.
32 O. Bumbu, C. Ceamanos, O. Crespo, M. C. Gimeno, A. Laguna, C. Silvestru and M. D. Villacampa, *Inorg. Chem.*, 2007, **46**, 11457-11460.
33 N. V. Kirij, W. Tyrra, D. Naumann, Y. L. Yagupolskii, I. Pantenburg and M. Schäfer, *J. Fluor. Chem.*, 2004, **125**, 1933-1938.
34 R. Usón, A. Laguna, M. Laguna, B. R. Manzano, P. G. Jones and G. M. Sheldrick, *J. Chem. Soc., Dalton Trans.*, 1984, DOI: 10.1039/DT9840000839, 839-843.
35 M. C. Gimeno and A. Laguna, *Chem. Rev.*, 1997, **97**, 511-522.
36 P. Pyykkö and M. Atsumi, *Chem. Eur. J.*, 2009, **15**, 186-197.
37 Z. Gan, Y. Lin, L. Luo, G. Han, W. Liu, Z. Liu, C. Yao, L. Weng, L. Liao, J. Chen, X. Liu, Y. Luo, C. Wang, S. Wie and Z. Wu, Angew. Chem., Int. Ed., 2016, **55**, 11567-11571.
38 S. Takano, H. Hirai, T. Nakashima, T. Iwasa, T. Taketsugu and T. Tsukuda, *J. Am. Chem. Soc.*, 2021, **143**, 10560-10564.
39 J. P. A. Souza, L. R. A. Menezes, F. P. Garcia, D. B. Scariot, P. T. Bandeira, M. B. Bespalhok, S. O. K. Giese, D. L. Hughes, C. V. Nakamura, A. Barison, A. R. M. Oliveira, R. B. Campos and L. Piovan, *Chem. Eur. J.*, 2021, **27**, 14427-14437.
40 M. J. Harper, E. J. Emmett, J. F. Bower and C. A. Russell, *J. Am. Chem. Soc.*, 2017, **139**, 12386-12389.

View Article Online
DOI: 10.1039/D5DT02489G

Supplementary information: Figure S2: UV/VIS spectrum of the CHCl3 solution prior crystallization, Figures S3 and S4, solid state NMR data, Figures S5-S8, mass spectrometric data, Figure S9: - DRIFT-spectrum of 1, Figure S10: TG/DTA data of 1, Tables S1 and S2 and Figure S11 and S12- 14, results of SEM and EDX measurements, table S3 crystallographic parameters of 1. The supplementary crystallographic data (CCDC 2483370) can be obtained online free of charge at www.ccdc.cam.ac.uk/conts/retrieving.html or from Cambridge Crystallographic Data Centre, 12 Union Road, Cambridge CB21EZ; Fax: (+44)1223-336-033; or deposit@ccdc.cam.ac.uk.